Indazole *N*-oxide derivatives as antiprotozoal agents: Synthesis, biological evaluation and mechanism of action studies

Alejandra Gerpe,[a] Gabriela Aguirre,[a] Lucía Boiani,[a] Hugo Cerecetto,[a,*]
Mercedes González,[a,*] Claudio Olea-Azar,[b] Carolina Rigol,[b] Juan D. Maya,[c]
Antonio Morello,[c] Oscar E. Piro,[d] Vicente J. Arán,[e] Amaia Azqueta,[f]
Adela López de Ceráin,[f] Antonio Monge,[f] María Antonieta Rojas[g] and Gloria Yaluff[g]

[a]*Departamento de Química Orgánica, Facultad de Química-Facultad de Ciencias, Universidad de la República,
Iguá 4225, Montevideo 11400, Uruguay*
[b]*Departamento de Química Inorgánica y Analítica, Facultad de Ciencias Químicas y Farméuticas,
Universidad de Chile, Olivos 1007, 233 Santiago, Chile*
[c]*Departamento de Farmacología Clínica Molecular, Facultad de Medicina, Universidad de Chile, PO Box 70000, 7 Santiago, Chile*
[d]*Departamento de Física, Facultad de Ciencias Exactas, Universidad Nacional de La Plata-Instituto IFLP(CONICET),
C.C. 67, 1900 La Plata, Argentina*
[e]*Instituto de Química Médica (CSIC), Juan de la Cierva 3, 28006 Madrid, Spain*
[f]*Centro de Investigación en Farmacobiología Aplicada, Universidad de Navarra, Irunlarrea s/n,
31080 Pamplona, Navarra, España, Spain*
[g]*Instituto de Investigaciones en Ciencias de la Salud, Dpto. de Medicina Tropical, Universidad Nacional de Asunción,
Río de la Plata y Lagerenza, Asunción, Paraguay*

Abstract—A series of indazole *N*-oxide derivatives have been synthesized and their antichagasic and leishmanocidal properties studied. 3-Cyano-2-(4-iodophenyl)-2*H*-indazole N^1-oxide exhibited interesting antichagasic activity on the two parasitic strains and the two parasitic stages evaluated. Furthermore, besides its trypanocidal activity, 3-cyano-2-(4-nitrophenyl)-2*H*-indazole N^1-oxide showed leishmanocidal activity in the three parasitic strains evaluated. To gain insight into the mechanism of action, electrochemical behaviour, ESR experiment, inhibition of parasitic respiration and QSAR were performed.

1. Introduction

Parasitic diseases are the foremost worldwide health problem today, particularly in the underdeveloped countries. In South America, Chagas' disease occupies the third place in number of deaths per year, after malaria and schistosomiasis.[1–4] *Trypanosoma cruzi* (*T. cruzi*) the aetiological agent of this illness, possesses a complex cycle of life that does not permit to obtain an efficient drug. Only two drugs are commercially available for the treatment of this disease, Nifurtimox (Nfx, currently discontinued) and Benznidazole (Bnz), being these chemotherapeutic agents still inadequate due to their undesired side effects.[3]

On the other hand, the leishmaniases are a series of diseases caused by *Leishmania* species. There are approximately 1.5 million cases of leishmaniases each year from Central and South America, West Asia and Europe.[5] The drugs, which have been most frequently used to treat the leishmaniases, are the pentavalent antimonials, Pentostam and Glucantime.[6] However, these drugs are quite toxic and in some areas resistance can be as high as 40%.[7] Currently, WHO/TDR is developing a research programme with Miltefosine, a very promising leishmanocidal drug, but new therapeutic alternatives should be found in order to increase the pharmaceutical arsenal.
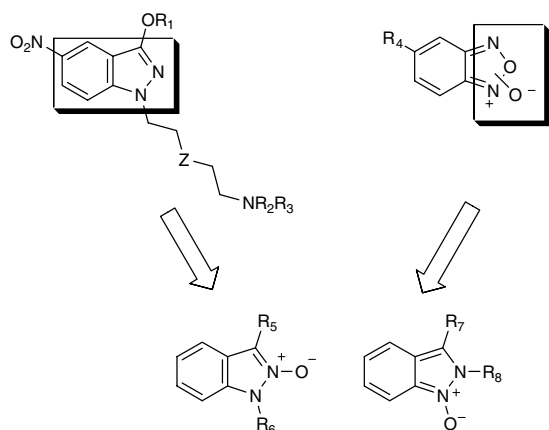
Chart 1. Design concept of indazole *N*-oxide as antiprotozoal agents.

Recently, we have studied in vitro antichagasic and anti-trichomona activity of 5-nitroindazoles, showing remarkable antiprotozoal properties in both parasites.[8] We found that in this family of compounds the nitro moiety did not play a crucial role in the trypanocidal activity.[8b] On the other hand, we have found that certain *N*-oxide containing heterocycles displayed excellent trypanocidal activity.[9] The well-known *N*-oxide bio-reduction process and its biological consequences[10] were found as crucial steps in the trypanocidal activity displayed by this group of compounds. This turns the *N*-oxide moiety as an excellent pharmacophore. These facts prompted us to propose a new potential antiprotozoal entity, which combines indazole system and *N*-oxide moiety (Chart 1). Biological behaviour of these heterocyclic systems has not been reported yet. Therefore, we studied the indazole *N*-oxide derivatives as new antiprotozoal agents.

Herein, we report the synthesis of indazole N^1- and N^2-oxide derivatives and their antiprotozoa activity (against *T. cruzi*, *Leishmania amazonensis*, *Leishmania infantum* and *Leishmania braziliensis*). Also, we present the electrochemical and ESR studies that allowed to explain their biological behaviour. Moreover, we study the modification in the uptake of oxygen promoted by indazole. Finally, we developed a QSAR study.

2. Methods and results

2.1. Synthesis

The indazole N^1-oxide derivatives were prepared following the pathways showed in Scheme 1. The synthetic route described for the preparation of this system involves the formation of the Schiff base between 2-nitrobenzaldehyde and the corresponding amines. Treatment with sodium cyanide converts the Schiff base to its α-aminonitrile derivatives, which in turn undergo basic cyclization.[11] The cyclization occurs under extremely mild condition and indazole N^1-oxide yield depends on the reaction solvent, being acetic acid the best condition.[12] We applied successfully this methodology to derivatives **1**–**8**, using Et₃N as base and to derivative **9** using NaHCO₃. For derivatives **10**–**13**, acidic conditions yielded the indazole N^1-oxide spontaneously. When we used 4-aminomorpholine as nucleophile, the corresponding α-aminonitrile derivative was not generated because the hydrazone moiety was not susceptible to the cyanide nucleophilic attack, yielding 4-(2-nitrobenzylideneamino)morpholine (**14a**. Scheme 2). Attempts to reduce this hydrazone moiety were performed in different conditions. In mild conditions, namely NaBH₄, the system did not react. However, when we used a strong reductant, LiAlH₄, a very complex mixture of reaction products was obtained. As a marginal product the indazole N^1-oxide **14** was identified (by ¹H NMR spectroscopy). No further attempts were performed to improve the preparation of **14**. Indazole N^2-oxide, derivative **15**, was synthesized following the procedure described by Zenchoff et al. (Scheme 2).[13]
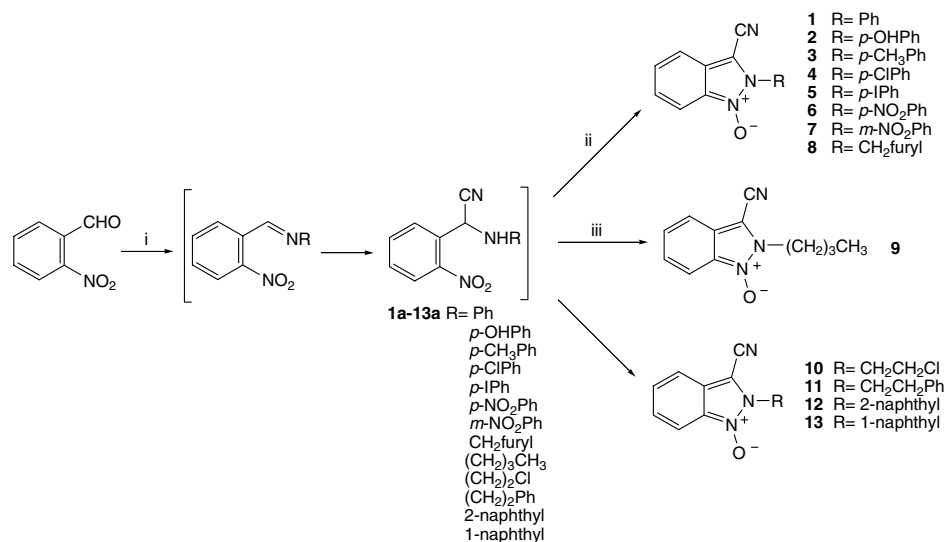

**Scheme 1.** Reagents and conditions: (i) H₂NR, KCN, CH₃CO₂H, rt. (ii) Et₃N, rt. (iii) NaHCO₃, rt.
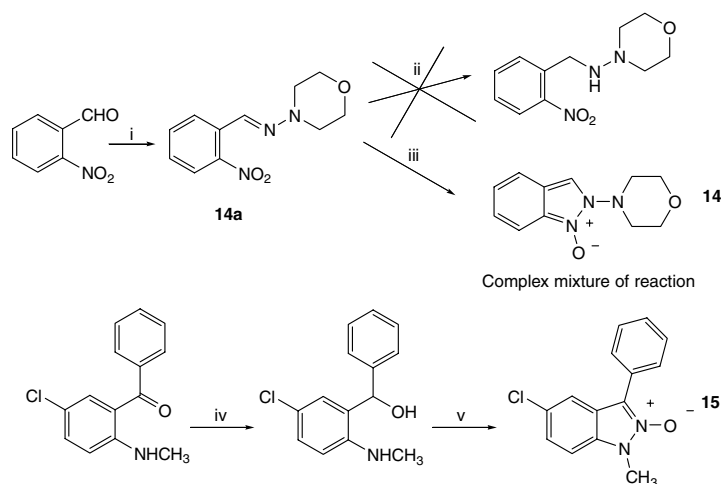
Scheme 2. Reagents and conditions: (i) 4-aminomorpholine, KCN, CH_3CO_2H, rt. (ii) $NaBH_4$, MeOH, reflux. (iii) $LiAlH_4$, THF, rt. (iv) $NaBH_4$, MeOH, rt. (v) 1—$NaNO_2$, HCl (concd); 2—H_2SO_4 (concd), rt.

In order to investigate the relevance of the *N*-oxide moiety in the biological behaviour, we synthesized three deoxygenated derivatives (**16**–**18**) (Scheme 3).[14] These derivatives were obtained with moderate yield treating the corresponding indazole N^1-oxide with PPh_3.

All new compounds were characterized by NMR (^{1}H-, ^{13}C-, HMQC and HMBC), MS and IR analysis and their purity established by TLC and microanalysis. Single crystals of derivative **13** adequate for structural X-ray diffraction studies[15] were obtained by slow evaporation from an EtOH solution. Figure 1 shows the ORTEP molecular drawing of derivative **13**.

16 R=*p*-OHPh
17 R=*p*-IPh
18 R=*p*-NO$_2$Ph
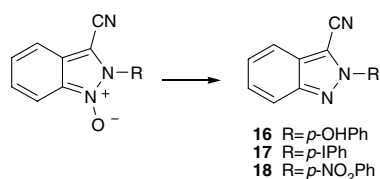
Scheme 3. Reagents and condition: PPh_3, EtOH, reflux.
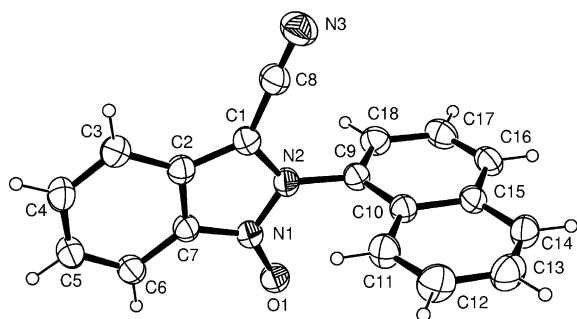
Figure 1. Molecular plot of derivative **13** showing the labelling of the non-H atoms and their displacement ellipsoids at the 30% probability level.

2.2. Biological characterization

2.2.1. Antitrypanosomal activities. All the compounds were tested in vitro against two parasitic strains (Brener and Tulahuen 2) and two parasitic stages (epimastigote and trypomastigote forms) of *T. cruzi* at different concentrations. Table 1 shows the percentage of growth

Table 1. In vitro antichagasic activity of Indazole *N*-oxide derivatives

Compound	Epimastigote growth inhibition (% GI)[a,b]		Trypomastigote reduction[b,c]
	Brener strain	Tulahuen strain	Brener strain
1	13	5	31
2	1	25	67
3	16	5	ND[d] (53)[e]
4	39	53	0 (0)
5	46	51	61
6	79 (16.2)[f]	70 (16.7)[f]	0
7	47	52	ND (39)[e]
8	12	49	34
9	0	13	ND (59)[e]
10	0	0	ND
11	31	23	7
12	16	25	26
13	52	44	0 (12)[e]
15	0	21	ND
16	4	33	6 (40)[e]
17	3	17	ND (59)[e]
18	12	34	ND (29)[e]
Nfx	99 (8.5)[f]	100 (7.7)[f]	—
GV[g]	—	—	100

[a] Values expressed as the percentage of inhibition of control growth (% GI). Compounds tested at 25 μM concentration.
[b] Results are means of three different experiments with SD less than 10% in all cases.
[c] Values correspond to the percentage of reduction of control trypomastigotes. Compounds tested at 100 μg/mL.
[d] Not determined.
[e] Values in parentheses correspond to the inhibition using 250 μg/mL of each compound.
[f] Values in parentheses correspond to the IC$_{50}$ (μM).
[g] GV, gentian violet.

inhibition (% GI) of the indazole derivatives at 25 μM for the epimastigote form and at 100 or 250 μg/mL for the bloodstream form, trypomastigote. From concentration–activity curves the most active derivative against both epimastigote strains was **6** with IC_{50} values in the same order as that of the reference drug (Nfx).

Compounds **4**, **5**, **7** and **13** showed medium activity at the assayed concentrations against the two studied strains, while compound **8** showed moderated activities against both forms, epimastigote of Tulahuen and trypomastigote of Brener. Derivatives **2** and **5** were the most active derivatives against trypomastigote form. Derivative **5** also showed remarkable antiprotozoal properties against both epimastigote and trypomastigote forms. In general, the antiepimastigote activities of the studied derivatives were slightly higher for Tulahuen than for Brener strain, results which are similar to those previously reported for nitroimidazoles.[16] In general, the anti-*T. cruzi* activities (on epimastigote and trypomastigote forms) of the deoxygenated derivatives **16–18** decreased compared with those of their *N*-oxide analogues, indicating that the presence of the *N*-oxide group is important for the antichagasic activity.

2.2.2. Leishmanocidal activities. According to their behaviour against epimastigote and trypomastigote forms of *T. cruzi*, we selected three different indazole *N*-oxides for evaluation as leishmanocidal agents, the two most actives against bloodstream form (**2** and **5**) and the most active against epimastigote form (**6**). Derivatives **2**, **5** and **6** were tested in vitro against promastigote forms of *L. amazonensis*, *L. infantum* and *L. braziliensis* strains at 100 μg/mL (Table 2). Derivative **6** was the most active compound against these strains, showing an immobility or decrease of the growth of parasites that corresponds to 70–90% of parasite lysis.

2.2.3. Cytotoxic activity. According to their behaviour against the bloodstream form, we selected four different indazole *N*-oxides, the most active (**5**), one mid-active (**1**), and two inactive derivatives (**3** and **4**), for evaluation as mammal cytotoxic agents. Then, these compounds were tested against three tumour cell lines, human colon adenocarcinoma (HT-29), human mammary adenocarcinoma (MCF-7) and human kidney carcinoma (TK-10) at 100 μM. Cell survival percentages (% SP) are gathered in Table 3. None of the tested compounds

Table 3. Cytotoxicity to MCF-7, TK-10 and HT-29 cell lines at 100 μM

Compound	% SP[a]		
	MCF-7	TK-10	HT-29
1	86	88	95
3	83	89	100
4	79	84	86
5	87	83	100

[a] % SP, cell survival percentage.

showed antineoplastic activity since the survival of the three cell lines was very high.

2.3. Study of anti-*T. cruzi* mechanism of action

In order to confirm an oxidative stress-mediated mechanism of action, we performed some experiments related to this fact. We studied the *N*-oxides' electrochemical behaviour, the production of free radicals induced by the studied compounds into the parasite by ESR experiments and the compounds effect on the parasitic oxygen consumption.

2.3.1. Electrochemical behaviour. We performed voltammetric studies in DMSO solutions, analysing the first reduction peak for the *N*-oxide derivatives. Table 4 lists the values of the first voltammetric cathodic peaks for all compounds and Nfx.[17] The *N*-oxide reduction occurred between −1.3 and −1.6 V with the absence of anodic peak, thus indicating an electron irreversible transfer process. In the case of derivatives **6** and **7** which possess in their structures a nitro group, two extra reduction peaks appeared. The first, near −0.9 V, corresponds to one-electron reversible transfer process that is attributed to the generation of the nitro anion radical. The second peak corresponds to the reduction of the nitro anion radical to the hydroxylamine by a three-electron process.[18] The cathodic peaks of derivatives **1–13** corresponding to *N*-oxide reduction are irreversible in the whole range of sweep rates used (0–2000 mVs⁻¹) and involved one electron.[19] We attributed this feature

Table 2. Leishmanocidal activity

Compound	*L. amazonensis*[a]	*L. infantum*[a]	*L. braziliensis*[a]
2	+	+	+
5	+	+	+
6	++	++	++
Pentamidine	+++	+++	+++
DMSO	0	0	0

+++, total lysis of parasites (100% of lysis); ++, immobility or decrease of the growth of parasites (between 70% and 90% of lysis of parasites); +, similar growth of parasites to the control but with little mobility; 0, lysis of parasites is not observed. Initial inocula, 2×10^6 parasites/mL.
[a] At 100 μg/mL.

Table 4. Cyclic voltammetric parameters in DMSO versus saturated calomel electrode (sweep rate 2 Vs⁻¹)

Compound	E_{pc}[a] (V)
1	−1.33
2	−1.36
3	−1.36
4	−1.28
5	−1.26
6	−0.92
7	−0.98
8	−1.47
9	−1.61
11	−1.55
12	−1.27
13	−1.35
Nfx	−0.91[b]

[a] E_{pc}, potential of the first cathodic peak.
[b] Ref. 17.
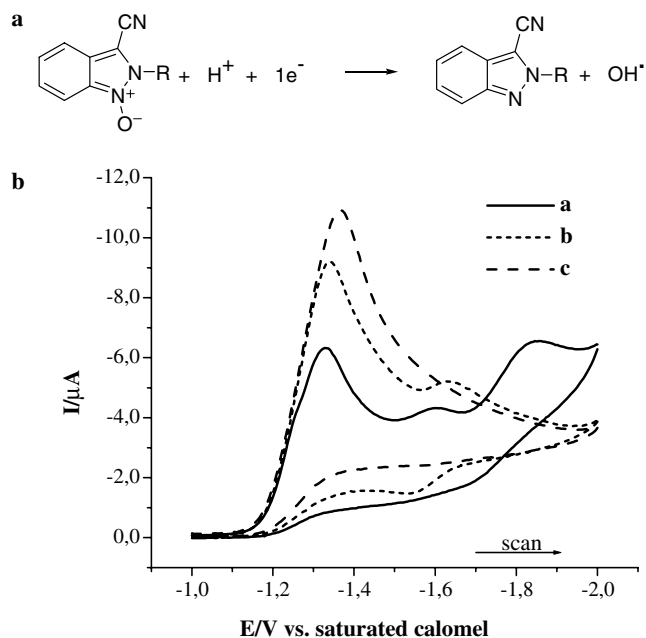
Figure 2. (a) Reduction mechanism proposed to *N*-oxide derivatives. (b) Cyclic voltammograms in DMSO: (a) derivative **1**, (b) GSH: derivative **1** (1:1) and (c) GSH:derivative **1** (2:1).

to the production of the deoxygenated derivative with hydroxyl radical release (Fig. 2a).

The electrochemical properties of these compounds in the presence of a biologically relevant thiol, glutathione (GSH), have been studied. According to a previous report, this thiol could biologically act as a radical scavenger, an oxidizing or a reducing agent, or it is able to display all these three functions depending on the conditions.[20,21] We studied the reactivity of GSH with the radical of indazole N^1-oxide by cyclic voltammetry, adding increasing amounts of aqueous GSH solution (0.1 M in phosphate buffer, pH 7.4) to the medium. Figure 2b shows the typical cyclic voltammograms of derivatives in DMSO solution in the absence and in the presence of increasing amounts of GSH. Curve (a) illustrates the cyclic voltammogram that involves the reduction process of derivative **1**. Afterwards, when GSH was added to the medium, it produces a significant increase in the first cathodic current with a concomitant displacement to low potential and decreasing of the second cathodic peak (curve (b)). After the addition of GSH in ratio GSH: derivative (2:1), only the first cathodic peak appeared (curve (c)). The GSH signals, at the studied concentrations, did not interfere with the signals of the corresponding *N*-oxide.

These electrochemical behaviours suggest that a new electro-active entity was formed by reaction of the indazole *N*-oxide and GSH. This could show that the radical of the *N*-oxide species chemically reacts with GSH.

2.3.2. ESR spectroscopic studies. In order to analyse the capacity of these compounds to generate free radicals
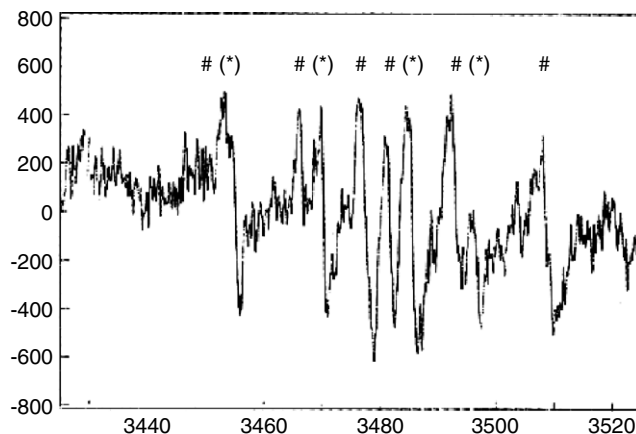
Figure 3. ESR spectrum obtained with *T. cruzi* extracts incubated with derivative **5**. The ESR signals were observed 10 min after incubation at 37 °C with *T. cruzi* extract (4 mg protein/mL), NADPH (1 mM), EDTA (1 mM), in phosphate buffer (20 mM), pH 7.4, DMPO (100 mM) and **5** (2 mM in acetonitrile). Spectrometer conditions: microwave frequency 9.68 GHz microwave power 20 mW, modulation amplitude 0.4 G, scan rate 0.83 G/s, time constant 0.25 s and number of scan: 10.

in vivo, we incubated derivative **5** with *T. cruzi* homogenates in the presence of NADPH, EDTA and the spin trapping DMPO.[22] A well-resolved ESR spectrum appeared when DMPO was added to the *T. cruzi*–**5** system. In this ESR spectrum, it was possible to observe the corresponding trapped hydroxyl radical (DMPO-OH spin adduct $a_N = a_H = 15.09$ G, Figure 3 marked (*)).[22b] Furthermore, other six lines appeared that were consistent with the trapped *N*-oxide radical according to the hyperfine pattern and the hyperfine constants ($a_N = 15.84$ G, $a_H = 25.90$ G, Figure 3 marked #).[22a] These results are in agreement with the electrochemical behaviour of indazole *N*-oxide derivatives, when the system is mono-electronated the hydroxyl radical is released.

2.3.3. Effect on the parasitic respiration. Derivatives **1**, **3**, **5** and **6** were selected to be tested for their capacity to inhibit parasitic respiration. These derivatives were chosen taking into account their anti-*T. cruzi* activities, **1** and **3** being inactive compounds and **5** and **6** active. These experiments afforded to investigate the products' ability to produce oxidative stress. Respiration measurements were carried out polarographically treating *T. cruzi* (epimastigote form, Tulahuen 2 strain) with different concentrations of the studied compounds (Table 5).[17c] These derivatives inhibited oxygen uptake in a concentration-dependent manner (for derivative **6** it was not possible to perform concentration–response studies because **6** precipitates in the experimental conditions). Only derivative **5** inhibited respiration close to 30% at IC_{50} equivalent concentration (see Section 5).

The studied compounds were unable to produce redox cycling. These results confirm that the hydroxyl radical observed in the ESR experiments could be the result of OH·-releasing capacity of compounds after a bio-reduction process.

Table 5. Effect of indazole *N*-oxide derivatives on respiration of *T. cruzi*

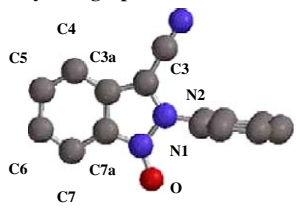| Compound	IC$_{50}$ (μM) [a]	Inhibition of respiration[b]
1	>100	0.0 ± 5.5
3	>100	16.7 ± 4.8
5	25.1	27.2 ± 4.8
6	16.7	5.5 ± 4.9

[a] IC$_{50}$ values for Tulahuen strain.
[b] Values are expressed as the percentage with respect to control and correspond to means ± standard deviation of three independent experiments. Compounds added at a final concentration equal to IC$_{50}$ equivalent concentrations (see Section 5). Control respiration was 31.5 nanoatoms of oxygen per minute and per milligram of protein.

2.4. Structure–activity relationships

Molecular modelling studies were performed on the developed indazole N^1-oxide derivatives by calculating the stereoelectronic properties in order to understand the mechanism of action. These properties were determined using DFT/B3LYP calculations.[23,24] A detailed conformational search for each of the molecules was performed, using MM methods, to find the minimum energy and highest abundance conformer. The geometry of this conformer was fully optimized by applying PM3/6-31G* in the gas phase that allows us to obtain acute results with low time of computational calculi. Then, single point B3LYP/6-31G* density functional calculation was performed. The crystallographic molecular structure of derivative **13** was used as template in order to assess the validity of the theoretical level used. As shown in Table 6, PM3/6.31G* geometry describes adequately bond distances and angles and also dihedral angles. The properties determined and examined in this study were total energy, solvation (water) energy, magnitude of dipolar moment, volume, HOMO's and LUMO's energies, gap (E_LUMO–E_HOMO) and the logarithm of the partition coefficient of the non-ionized molecules (log P). Theoretical log P (clog P) was calculated using the Villar method, implemented in PC SPARTAN 04 package[24] at the PM3 semiempirical level.

In the equations and models, *n* represents the number of data points, r^2 is the correlation coefficient, *s* is the standard deviation of the regression equation, the *F* value is related to the *F*-statistic analysis (Fischer test) and r^2adj defines the cross-validated correlation coefficient. Activity used in the structure–activity relationship studies was the inhibitory effect (compounds **1**–**13**) on the growth of *T. cruzi* (Brener and Tulahuen strains) expressed as the percentage of growth inhibition at day 5 at 25 μM concentration, % GI. We used log$_{10}$ (GI) values as the dependent variables in the linearization procedure. First, one-variable and multivariable regressions between both activities and the physicochemical properties (calculated descriptors and redox potential) were studied. Non-statistical significant correlations were obtained when E_{pc} was included as independent variable, but it was observed a clear tendency between activities and redox potential, namely the most active compounds possess the least negative E_{pc} (Fig. 4). This could indi-

Table 6. Crystallographic and PM3/6.31G* optimized structure of compound **13**

Crystallographic structure   **PM3/6.31G* optimised structure**

13

Distances and angles[a,b]	Crystallographic data	PM3/6.31G* optimized geometry	Relative error $\|(d_{PM3/6.31G^*}-d_{crist})/d_{crist}\|$
O–N1	1.270	1.257	0.01
N1–N2	1.408	1.380	0.02
N2–C3	1.368	1.389	0.02
C3–C3a	1.467	1.404	0.25
C3a–C4	1.437	1.417	0.01
C3a–C7a	1.409	1.420	0.01
C4–C5	1.418	1.377	0.03
C6–C7	1.378	1.376	0.00
C7–C7a	1.466	1.408	0.04
C7a–N1	1.398	1.370	0.02
O–N1–N2	120.95	122.92	0.02
N1–N2–C3	108.25	110.03	0.02
N2–C3–C3a	107.54	107.03	0.00
C3–C3a–C7a	107.38	106.52	0.01
C3a–C4–C5	119.63	118.06	0.01
C5–C6–C7	119.73	121.35	0.01
C7–C7a–C3a	123.35	123.26	0.00
N1–C7a–C3a	106.69	109.11	0.02

[a] Distances in Å and angles in °.
[b] Numbers according to figure.
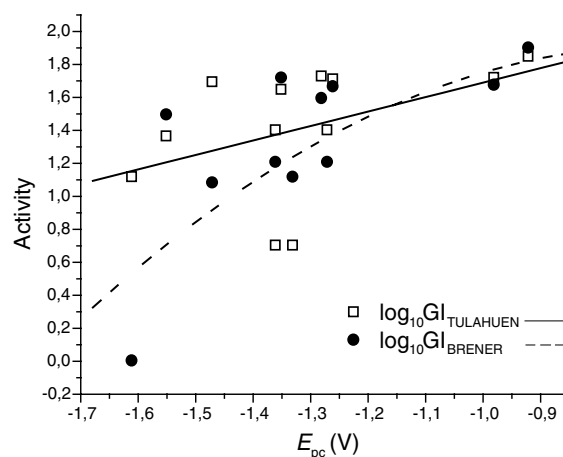
Figure 4. Potential of the first cathodic peak (E_{pc}) versus activities.

cate that other the properties participate in the displayed activities.

Only structure–activity models having a value of r^2adj above 0.5 were considered. In the case of trypanocidal activity against Brener strain, the best equation was obtained when we analysed the correlation between activity and the independent clog P and the magnitude

of dipolar moment, μ (Eq. 1, Table 7). Dipolar moments of derivatives are oriented with similar directions (Fig. 5a). For the same strain another statistical accepted correlation was obtained between the activities and $\text{clog}\,P$ and E_HOMO (Eq. 2). E_HOMO and μ magnitude are not orthogonal,[25] indicating that equations 1 and 2 present the same kind of results. Figure 5b shows the distribution of HOMO. In the case of trypanocidal activity against Tulahuen strain, the correlations were statistically less indicative than in the case of the Brener strain. However, like in the Brener strain the two best results were obtained with μ (Eq. 3, Table 7) and E_HOMO (Eq. 4) but in these cases with volume instead of $\text{clog}\,P$. $\text{clog}\,P$ and volume are not orthogonal,[25] indicating that equations 3 and 4 present the same kind of results. Figure 6 shows the plot of experimental activity versus calculated ones for Eq. 1–4. Besides, the correlation matrix for the used physicochemical descriptors was performed and cross-correlations between the descriptors used in each equation were not obtained.[25] These parameters are therefore orthogonal, a fact that affords their use in the multilinear regression procedure.[26]

3. Discussion

New indazole N^1-oxide derivatives were synthesized by a simple methodology and with good yields. Antiprotozoal activity, anti-*T. cruzi* and antileishmania, of indazole *N*-oxide derivatives has been reported for the first time. Some of them showed good anti-*T. cruzi* activity with low cytotoxicity. In particular, three of the studied derivatives (**4**–**6**) showed interesting properties. Compound **6** exhibited remarkable antiepimastigote activity, but did not show antitrypomastigote activity. Compounds **4** and **5** displayed antiepimastigote activity, and derivative **5** maintained trypanocidal activity in bloodstream form (trypomastigote). As it has been previously observed,[9a,9d,9e,27] the absence of the *N*-oxide moiety produces the drop of antiepimastigote activity, confirming that this group plays a key role in the mechanism of indazole *N*-oxides' antitrypanosomal activity (compare the activity of derivative **6** with the activity of deoxy-derivative **18**, Table 1). Derivative **6** displayed good activity against the three studied *Leishmania* strains, producing between 70% and 90% of parasite lysis. The antiprotozoal activity is not due to cytotoxicity since at the assayed concentration the compounds did not show a cytotoxic activity against mammary cells (Table 3).

Some important pieces of information were achieved from the experiments performed in order to clarify the mechanism of anti-*T. cruzi* activity. From the electrochemical studies it is possible to conclude that the *N*-oxide reduction is an irreversible process, indicating that the production of OH radical (Fig. 2a) could take place in the biological medium. However, a statistical correlation between activity and values of E_{pc} was not obtained

Table 7. Summary of QSAR results

| Equation	Statistic parameters						Expressions
	r^2adj	r^2	s	p	F value	n	
1	0.780	0.820	0.294	0.0004	20.49	12	$\log_{10}(\text{GI}_{\text{BRENER}}) = -3.63(\pm0.84) + 0.33(\pm0.06)\,\mu\ 0.73(\pm0.14)\,\text{clog}\,P$
2	0.734	0.782	0.323	0.0010	16.18	12	$\log_{10}(\text{GI}_{\text{BRENER}}) = -19(\pm4)\ -3.04(\pm0.67)\,\text{E}_{\text{HOMO}} + 0.71(\pm0.15)\,\text{clog}\,P$
3	0.573	0.679	0.356	0.0130	6.36	13	$\log_{10}(\text{GI}_{\text{TULAHUEN}}) = -19(\pm10) + 0.14(\pm0.08)\,\mu\ 0.15(\pm0.08)\,\text{vol}\ -0.0003(\pm0.0001)\,\text{vol}^2$
4	0.533	0.650	0.372	0.0190	5.56	13	$\log_{10}(\text{GI}_{\text{TULAHUEN}}) = -27(\pm10)\ -1.09(\pm0.76)\,\text{E}_{\text{HOMO}} + 0.17(\pm0.08)\,\text{vol}\ -0.0003(\pm0.0001)\,\text{vol}^2$
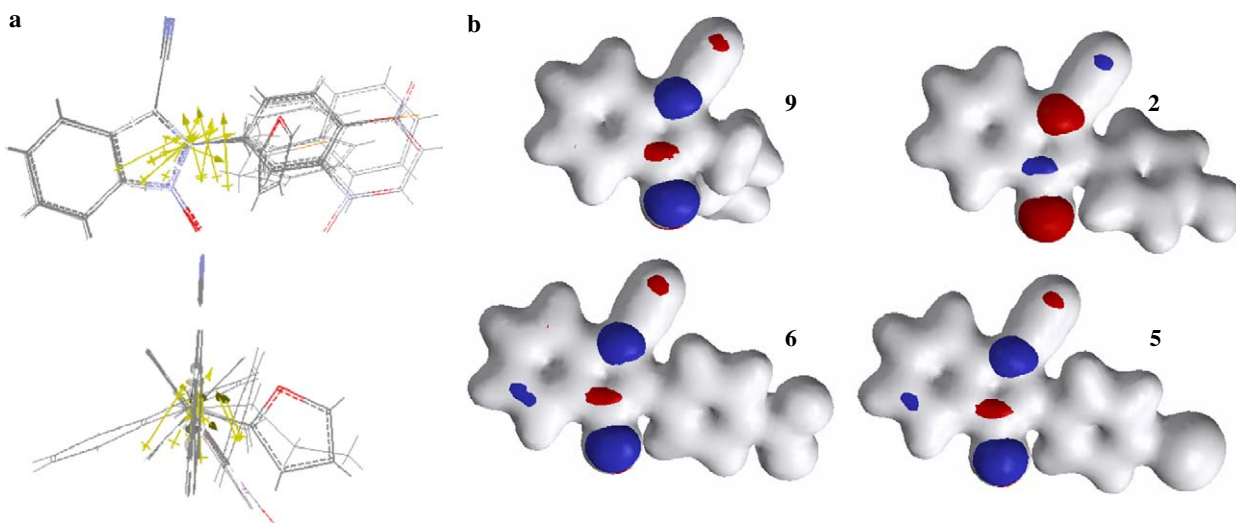
Figure 5. (a) Two different views of the dipoles of the studied indazole N^1-oxide derivatives. (b) Electron density (solid white, isovalue = 0.02) and HOMO (solid, isovalue = 0.032) isosurfaces for active (down) and inactive (up) derivatives.
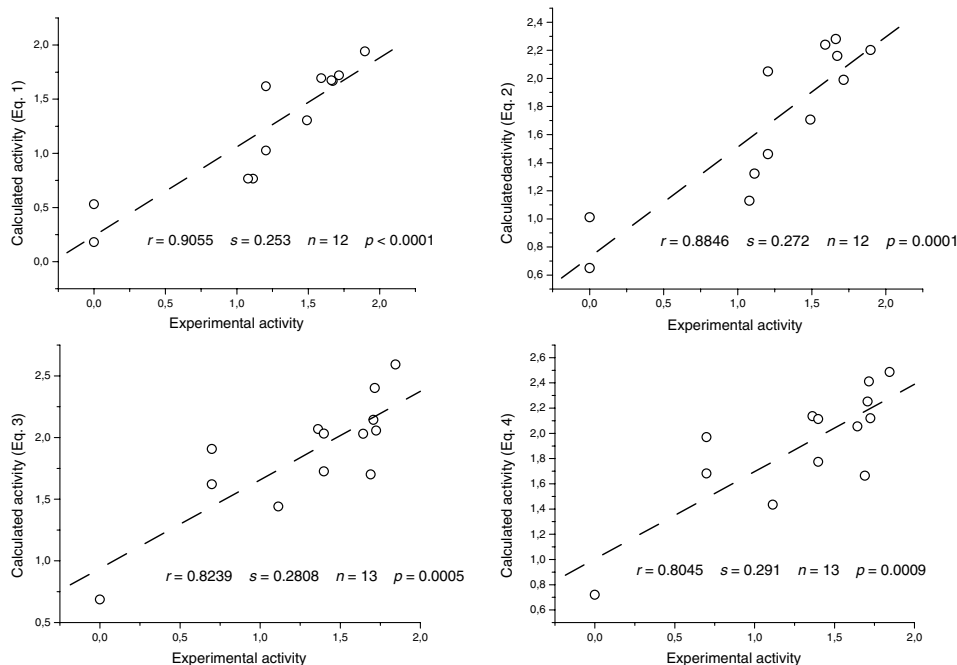
Figure 6. Plot of $\log_{10}$ of percentage of trypanosome growth inhibition, Brener (up) and Tulahuen (down) strains, at 25 μM (log10% GI) experimental versus calculated values from Eqs. 1 to 4.

but only a soft tendency was observed (Fig. 4). On the other hand, the electrochemical study with GSH showed that the compounds could react with an electroactive compound trapping it. The presence of the new entity was supported by the increase of the cathodic peak current corresponding to the anion radical generated by the GSH addition. The ESR experiment was in agreement with this fact demonstrating that one of the most active derivatives (**5**, Fig. 3) is able to generate free radicals within the parasitic cells, where OH˙ was detected. In the studies of the derivatives' effect on the oxygen consumption of *T. cruzi*, we observed that compounds present a little oxygen uptake inhibition in a concentration-dependent manner without oxygen recycling.

QSAR studies demonstrated the relevance of the dipolar moment module, or E_HOMO, and lipophilic properties for the trypanocidal activity on Brener strain and dipolar moment module, or E_HOMO, and volume for the trypanocidal activity on Tulahuen strain. The relationships between activity and dipolar moment module could indicate the electronic requirements for the derivatives to have optimal interactions with a target biomolecule. Observing the directions and ways of dipolar moments (Fig. 5a) the system *N*-oxide and CN determined these orientations. In this sense, it was possible to note that the most active compounds against both strains, derivatives **5** or **6** (Fig. 5b), showed the highest HOMO's contribution on indazole oxygen, nitrogen and carbon 3-, 4- and 6-. These results indicate that the compounds could act as nucleophiles through these atoms reacting with electrophile biomolecules and producing damages into parasite cell.[28] As it is well known, drug lipophilicity and volume play significant roles in biological responses such as the transport of the drugs through the cell membrane.[29] According to QSAR stud-

ies, the trypanocidal activity of indazole *N*-oxides also depends on lipophilicity and molecular volume.

4. Conclusions

The results presented above indicate that indazole *N*-oxide system constitutes a starting point for further chemical modifications in order to improve the antiprotozoal, *T. cruzi* and *Leishmania*, activity. The results provide supporting evidence to stimulate further in vivo studies of these compounds in appropriate animal models of Chagas' disease.

5. Experimental

5.1. Chemistry

Compound **15** was prepared according to literature procedure.[13] All starting materials were commercially available research-grade chemicals and used without further purification. All solvents were dried and distilled prior to use. All the reactions were carried out in a nitrogen atmosphere. Melting points were determined on a Leitz Microscope Heating Stage Model 350 capillary apparatus and are uncorrected. ^{1}H NMR (400 MHz) and ^{13}C NMR (100 MHz) spectra were recorded on a Bruker DPX-400 spectrometer. The chemical shifts are reported in ppm from TMS (δ scale). *J* values are given in Hz. The assignments have been performed by means of different standard homonuclear and heteronuclear correlation experiments (HMQC and HMBC). Electron impact (EI) mass spectra were obtained at 70 eV on a Shimadzu GC–MS QP 1100 EX instrument. IR spectra were recorded on a Perkin-Elmer 1310 spectrometer, using

potassium bromide tablets; the frequencies are expressed in cm^{-1}. DC-Alufolien silica gel 60 PF254 (Merck, layer thickness 0.2 mm) and silica gel 60 (Merck, particle size 0.040–0.063 mm) were used for TLC and flash column chromatography, respectively. Elemental analyses were obtained from vacuum-dried samples (over phosphorus pentoxide at 3–4 mm Hg, 24 h at room temperature) and performed on a Fisons EA 1108 CHNS-O analyser.

5.1.1. Synthesis of indazole N^1-oxide derivatives (1–8 and 10–13).

General method A (1–8). A mixture of *o*-nitrobenzaldehyde (0.50 g, 3.3 mmol), KCN (0.40 g, 6.6 mmol) and the corresponding amine (3.3 mmol) in glacial acetic acid (30 mL) was stirred at room temperature for 24 h. After addition of 20 mL water, the precipitated product was collected by filtration and air-dried. The solid (α-aminonitrile derivative) was treated with Et$_3$N (10 mL) and was stirred at room temperature for 24–48 h. After addition of 20 mL water the precipitated product was collected by filtration and air-dried, yielding the corresponding indazole N^1-oxide. The product was purified by crystallization from the indicated solvent.

General method B (10–13). A mixture of *o*-nitrobenzaldehyde (0.50 g, 3.3 mmol), KCN (0.40 g, 6.6 mmol) and the corresponding amine (3.3 mmol) in glacial acetic acid (30 mL) was stirred at room temperature for 36–48 h. After addition of 20 mL water, the precipitated product was collected by filtration and air-dried, yielding the corresponding indazole N^1-oxide. The product was purified by crystallization from the indicated solvent.

5.1.1.1. 3-Cyano-2-phenyl-2*H*-indazole N^1-oxide (1).
2-(2-Nitrophenyl)-2-phenylaminoacetonitrile (1a). Yellow solid 0.51 g (61%). ^{1}H NMR (400 MHz, DMSO-d_6) δ ppm: 6.44 (1H, d, $J = 9.8$ Hz), 6.78 (4H, m), 7.19 (2H, t, $J = 8.1$ Hz), 7.74 (1H, m), 7.90 (2H, m), 8.1 (1H, d, $J = 8.1$ Hz).

3-Cyano-2-phenyl-2H-indazole N^1-oxide (1). Yellow solid 0.29 g (62%) (method A); mp 193.6–194.3 °C (ethanol). ^{1}H NMR (400 MHz, DMSO-d_6) δ ppm: 7.50 (2H, m), 7.73 (3H, m), 7.85 (4H, m). ^{13}C NMR (100 MHz, DMSO-d_6) δ ppm: 92.42, 111.77, 115.06, 119.80, 123.04, 128.47, 128.81, 129.11, 129.66, 130.48, 132.07, 132.41. MS (EI, 70 eV) *m/z* (%): 235 (M$^+$, 75), 219 (M$^+$-16, 31), 206 (M$^+$-29, 26), 204 (8), 77 (100). IR (KBr, cm^{-1}): 2206, 1507, 1474, 1344, 1287, 1237, 1035, 865, 742. Anal. Calcd for C$_{14}$H$_9$N$_3$O (235.07): C 71.48; H 3.86; N 17.86. Found: C, 71.32; H, 3.95; N, 17.89.

5.1.1.2. 3-Cyano-2-(4-hydroxyphenyl)-2*H*-indazole N^1-oxide (2).
White solid 0.25 g (54%) (method A); mp 230.0–231.9 °C (methanol). ^{1}H NMR (400 MHz, DMSO-d_6) δ ppm: 7.03 (2H, d, $J = 8.8$ Hz), 7.48 (1H, dd, $J = 6.8$, 8.4 Hz), 7.52 (1H, dd, $J = 6.8$, 8.3 Hz), 7.57 (2H, d, $J = 8.8$ Hz), 7.81 (1H, d, $J = 8.4$ Hz), 7.85 (1H, d, $J = 8.3$ Hz), 10.34 (1H, br s). ^{13}C NMR (100 MHz, DMSO-d_6) δ ppm: 92.00, 112.00, 115.00, 116.84, 119.72, 122.69, 123.00, 128.24, 128.92, 129.45, 130.38, 160.89. MS (EI, 70 eV) *m/z* (%): 251 (M$^+$, 100); 235 (M$^+$-16, 24); 220 (M$^+$-31, 41); 93 (14). IR (KBr, cm^{-1}): 3500–3200, 2224, 1596, 1511, 1445, 1351,

1277, 1232, 1033, 821, 747. Anal. Calcd for C$_{14}$H$_9$N$_3$O$_2$ (251.07): C, 66.93; H, 3.61; N, 16.72. Found: C, 66.61; H, 4.00; N, 16.41.

5.1.1.3. 3-Cyano-2-(4-tolyl)-2*H*-indazole N^1-oxide (3).
2-(2-Nitrophenyl)-2-(4-tolylamino)acetonitrile (3a). Yellow solid 0.75 g (60%). ^{1}H NMR (400 MHz, DMSO-d_6) δ ppm: 2.19 (3H, s), 6.38 (1H, d, $J = 10.0$ Hz), 6.59 (1H, d, $J = 10.0$ Hz), 6.71 (2H, d, $J = 8.2$ Hz), 7.00 (2H, d, $J = 8.2$ Hz), 7.72 (1H, m), 7.86 (1H, m), 7.93 (1H, d, $J = 7.3$ Hz), 8.09 (1H, d, $J = 7.8$ Hz).

3-Cyano-2-(4-tolyl)-2H-indazole N^1-oxide (3). Yellow solid 0.25 g (74%) (method A); mp 203.0–205.0 °C (ethanol). ^{1}H NMR (400 MHz, DMSO-d_6) δ ppm: 2.46 (3H, s), 7.52 (4H, m), 7.80 (2H, d, $J = 8.2$ Hz), 7.84 (1H, d, $J = 6.6$ Hz), 7.86 (1H, d, $J = 8.4$ Hz). ^{13}C NMR (100 MHz, DMSO-d_6) δ ppm: 21.82, 92.42, 111.80, 115.03, 119.77, 122.92, 128.39, 128.56, 129.07, 129.52, 129.59, 130.92, 142.61. MS (EI, 70 eV) *m/z* (%): 249 (M$^+$, 100); 233 (M$^+$-16, 22); 219 (M$^+$-30, 22). IR (KBr, cm^{-1}): 2201, 1516, 1488, 1438, 1348, 1242, 1035, 809, 745. Anal. Calcd for C$_{15}$H$_{11}$N$_3$O (249.09): C, 72.28; H, 4.45; N, 16.86. Found: C, 72.08; H, 4.62; N, 16.80.

5.1.1.4. 2-(4-Chlorophenyl)-3-cyano-2*H*-indazole N^1-oxide (4).
2-(4-Chlorophenylamino)-2-(2-nitrophenyl)acetonitrile (4a). Brown solid 0.20 g (21%). ^{1}H NMR (400 MHz, DMSO-d_6) δ ppm: 6.45 (1H, d, $J = 9.5$ Hz), 6.82 (2H, d, $J = 8.6$ Hz), 6.99 (1H, d, $J = 9.5$ Hz), 7.23 (2H, d, $J = 8.6$ Hz), 7.67 (3H, m), 8.11 (1H, d, $J = 8.0$ Hz).

2-(4-Chlorophenyl)-3-cyano-2H-indazole N^1-oxide (4). Brown solid 0.29 g (62%) (method A); mp 202.5–203.2 °C (ethanol). ^{1}H NMR (400 MHz, DMSO-d_6) δ ppm: 7.52 (2H, m), 7.84 (6H, m). ^{13}C NMR (100 MHz, DMSO-d_6) δ ppm: 92.57, 111.70, 115.05, 119.82, 123.08, 128.59, 129.11, 129.75, 130.63, 130.76, 130.82, 137.27. MS (EI, 70 eV) *m/z* (%): 269 (M$^+$, 46); 253 (M$^+$-16, 7); 204 (29); 111 (57); 75 (100). IR (KBr, cm^{-1}): 2211, 1504, 1440, 1351, 1240, 1087, 1014, 821, 748. Anal. Calcd for C$_{14}$H$_8$ClN$_3$O (269.04): C, 62.35; H, 2.99; N, 15.58. Found: C, 62.15; H, 3.01; N, 15.44.

5.1.1.5. 3-Cyano-2-(4-iodophenyl)-2*H*-indazole N^1-oxide (5).
2-(4-Iodophenylamino)-2-(2-nitrophenyl)acetonitrile (5a). Yellow solid 0.71 g (57%). ^{1}H NMR (400 MHz, DMSO-d_6) δ ppm: 6.44 (1H, d, $J = 9.5$ Hz), 6.66 (2H, d, $J = 8.7$ Hz), 7.01 (1H, d, $J = 9.5$ Hz), 7.49 (2H, d, $J = 8.7$ Hz), 7.74 (1H, m), 7.87 (2H, m), 8.11 (1H, d, $J = 8.3$ Hz).

3-Cyano-2-(4-iodophenyl)-2H-indazole N^1-oxide (5). Yellow solid 0.30 g (64%) (method A); mp 212.8–213.3 °C (ethanol). ^{1}H NMR (400 MHz, DMSO-d_6) δ ppm: 7.49 (1H, dd, $J = 6.8$, 8.6 Hz), 7.54 (1H, dd, $J = 6.8$, 8.2 Hz), 7.62 (2H, d, $J = 8.4$ Hz), 7.83 (1H, d, $J = 8.6$ Hz), 7.87 (1H, d, $J = 8.2$ Hz), 8.11 (2H, d, $J = 8.4$ Hz). ^{13}C NMR (100 MHz, DMSO-d_6) δ ppm: 92.00, 99.82, 111.71, 115.05, 119.82, 123.11, 128.58, 129.00, 129.74, 130.67, 131.69, 139.43. MS (EI, 70 eV) *m/z* (%): 361 (M$^+$, 100); 345 (M$^+$-16, 7); 76 (9). IR

(KBr, cm^{-1}): 2210, 2198, 1503, 1439, 1351, 1243, 1035, 1010, 813, 744. Anal. Calcd for C$_{14}$H$_8$IN$_3$O (360.97): C, 46.56; H, 2.23; N, 11.64. Found: C, 47.06; H, 2.57; N, 11.52.

5.1.1.6. 3-Cyano-2-(4-nitrophenyl)-2*H*-indazole *N*^{1}-oxide (6). Yellow solid 0.30 g (63%) (method A); mp 223.1–224.3 °C (ethanol). ^{1}H NMR (400 MHz, DMSO-d_6) δ ppm: 7.52 (1H, dd, $J = 6.8$, 8.4 Hz), 7.57 (1H, dd, $J = 6.8$, 8.1 Hz), 7.86 (1H, d, $J = 8.4$ Hz), 7.90 (1H, d, $J = 8.1$ Hz), 8.17 (2H, d, $J = 8.9$ Hz), 8.56 (2H, d, $J = 8.9$ Hz). ^{13}C NMR (100 MHz, DMSO-d_6) δ ppm: 92.60, 111.59, 115.09, 119.90, 123.48, 125.69, 128.94, 129.33, 130.05, 130.24, 136.78, 149.70. MS (EI, 70 eV) m/z (%): 280 (M$^+$, 88); 264 (M$^+$-16, 7); 204 (71); 76 (100). IR (KBr, cm^{-1}): 2205, 1612, 1536, 1438, 1353, 1299, 1239, 1035, 845, 749. Anal. Calcd for C$_{14}$H$_8$N$_4$O$_3$ (280.06): C, 60.00; H, 2.88; N, 19.99. Found: C, 59.95; H, 2.74; N, 19.69.

5.1.1.7. 3-Cyano-2-(3-nitrophenyl)-2*H*-indazole *N*^{1}-oxide (7). *2-(2-Nitrophenyl)-2-(3-nitrophenylamino)acetonitrile (7a).* Brown solid 0.65 g (66%). ^{1}H NMR (400 MHz, DMSO-d_6) δ ppm: 6.64 (1H, d, $J = 9.1$ Hz), 7.24 (1H, dd, $J = 1.9$ Hz, $J = 8.0$ Hz), 7.91 (8H, m).

3-Cyano-2-(3-nitrophenyl)-2H-indazole N^1-oxide (7). Orange solid 0.14 g (30%) (method A); mp 207.1–208.0 °C (ethanol). ^{1}H NMR (400 MHz, DMSO-d_6) δ ppm: 7.48 (1H, dd, $J = 6.6$, 8.5 Hz), 7.52 (1H, dd, $J = 6.6$, 8.0 Hz), 7.77 (1H, d, $J = 8.0$ Hz), 7.89 (1H, d, $J = 8.5$ Hz), 7.91 (1H, dd, $J = 7.9$, 8.2 Hz), 8.17 (1H, d, $J = 7.9$ Hz), 8.54 (1H, d, $J = 8.2$ Hz), 8.68 (1H, s). ^{13}C NMR (100 MHz, DMSO-d_6) δ ppm: 92.00, 111.00, 115.08, 119.36, 123.15, 123.64, 126.37, 128.71, 129.00, 129.87, 131.29, 132.29, 133.07, 149.00. MS (EI, 70 eV) m/z (%): 280 (M$^+$, 100); 264 (M$^+$-16, 8); 250 (M$^+$-30, 4); 204 (8); 76 (18); 43 (87). IR (KBr, cm^{-1}):2207, 1536, 1503, 1440, 1353, 1276, 1237, 1167, 1114, 742. Anal. Calcd for C$_{14}$H$_8$N$_4$O$_3$ (280.06): C, 60.00; H, 2.88; N, 19.99. Found: C, 59.96; H, 2.78; N, 19.68.

5.1.1.8. 3-Cyano-2-(2-furylmethyl)-2*H*-indazole *N*^{1}-oxide (8). Yellow solid 0.19 g (24%) (method A); mp 143.2–144.8 °C (ethanol). ^{1}H NMR (400 MHz, CDCl$_3$) δ ppm: 5.78 (2H, s), 6.40 (1H, dd, $J = 1.8$, 3.2 Hz), 6.70 (1H, d, $J = 3.2$ Hz), 7.38 (1H, dd, $J = 6.7$, 7.4 Hz), 7.41 (1H, dd, $J = 6.7$, 7.6 Hz), 7.45 (1H, d, $J = 1.8$ Hz), 7.68 (1H, d, $J = 7.4$ Hz), 7.84 (1H, d, $J = 7.6$ Hz). ^{13}C NMR (100 MHz, CDCl$_3$) δ ppm: 42.29, 92.00, 111.42, 112.30, 112.44, 114.80, 119.18, 122.81, 127.68, 128.81, 129.00, 144.40, 145.50. MS (EI, 70 eV) m/z (%): 239 (M$^+$, 41); 222 (M$^+$-17, 7); 179 (45); 144 (14); 81 (100); 53 (100). IR (KBr, cm^{-1}): 2209, 1489, 1362, 1291, 1040, 777, 749. Anal. Calcd for C$_{13}$H$_9$N$_3$O$_2$ (239.07): C, 65.27; H, 3.79; N, 17.56. Found: C, 65.08; H, 4.04; N, 17.76.

5.1.1.9. 2-Butyl-3-cyano-2*H*-indazole *N*^{1}-oxide (9). A mixture of *o*-nitrobenzaldehyde (0.50 g, 3.3 mmol), KCN (0.40 g, 6.6 mmol) and butylamine (0.24 g, 3.3 mmol) in glacial acetic acid (30 mL) was stirred at room temperature for 24 h. The solution was treated with water (20 mL) and aqueous solution of NaHCO$_3$ (5%) until a basic pH was reached, and was stirred at room temperature for 48 h, precipitating a brown solid that was filtered, dried and purified by column chromatography (SiO$_2$, CH$_2$Cl$_2$). Brown solid 0.11 g (15%); mp 64.0–66.2 °C. ^{1}H NMR (400 MHz, DMSO-d_6) δ ppm: 0.91 (3 H, t, $J = 7.3$ Hz), 1.32 (2H, m), 1.84 (2H, m), 4.53 (2H, t, $J = 7.0$ Hz), 7.43 (1H, dd, $J = 6.9$, 7.8 Hz), 7.49 (1H, dd, $J = 6.9$, 7.5 Hz), 7.79 (1H, d, $J = 7.8$ Hz), 7.81 (1H, d, $J = 7.5$ Hz). ^{13}C NMR (100 MHz, DMSO-d_6) δ ppm: 14.13, 19.95, 30.39, 46.57, 91.30, 111.64, 114.69, 119.54, 122.34, 127.94, 129.19 (two carbons). MS (EI, 70 eV) m/z (%): 215 (M$^+$, 23); 198 (M$^+$-17, 26); 159 (100); 57 (14). IR (KBr, cm^{-1}): 2206, 1615, 1490, 1445, 1347, 1209, 1034, 745. Anal. Calcd for C$_{12}$H$_{13}$N$_3$O (215.11): C, 66.96; H, 6.09; N, 19.52. Found: C, 67.00; H, 6.23; N, 19.40.

5.1.1.10. 2-Chloroethyl-3-cyano-2*H*-indazole *N*^{1}-oxide (10). White solid 0.45 g (20%) (method B); mp 150.9–151.5 °C. ^{1}H NMR (400 MHz, CDCl$_3$) δ ppm: 4.09 (2H, t, $J = 5.7$ Hz), 4.90 (2H, t, $J = 5.7$ Hz), 7.43 (1H, dd, $J = 5.3$, 7.1 Hz), 7.46 (1H, dd, $J = 5.3$, 7.4 Hz), 7.72 (1H, d, $J = 7.1$ Hz), 7.84 (1H, d, $J = 7.4$ Hz). ^{13}C NMR (100 MHz, CDCl$_3$) δ ppm: 39.95, 48.40, 94.00, 110.50, 114.52, 119.28, 122.00, 128.00, 128.93, 129.00. MS (EI, 70 eV) m/z (%): 205 (M$^+$-16, 28); 143 (100); 88 (28); 77 (30); 63 (38). IR (KBr, cm^{-1}): 2361, 1684, 1601, 1489, 1424, 1300, 1266, 932, 758. Anal. Calcd for C$_{10}$H$_8$ClN$_3$O (221.04): C, 54.19; H, 3.64; N, 18.86. Found: C, 53.93; H, 3.33; N, 18.59.

5.1.1.11. 3-Cyano-2-phenethyl-2*H*-indazole *N*^{1}-oxide (11). White solid 0.17 g (20%) (method B); mp 120.6–121.7 °C (ethanol). ^{1}H NMR (400 MHz, CDCl$_3$) δ ppm: 3.30 (2H, t, $J = 7.2$ Hz), 4.80 (2H, t, $J = 7.2$ Hz), 7.20 (2H, d, $J = 8.0$ Hz), 7.31 (3H, m), 7.42 (2H, m), 7.63 (1H, d, $J = 8.4$ Hz), 7.87 (1H, d, $J = 8.8$ Hz). ^{13}C NMR (100 MHz, CDCl$_3$) δ ppm: 34.49, 48.32, 92.00, 110.52, 114.57, 119.13, 122.20, 127.62, 127.89, 128.63, 129.41, 129.43, 129.60, 136.19. MS (EI, 70 eV) m/z (%): 263 (M$^+$, 30); 247 (M$^+$-16, 2); 115 (9); 105 (100); 91 (39). IR (KBr, cm^{-1}): 2207, 1489, 1435, 1339, 1248, 1032, 822, 741. Anal. Calcd for C$_{16}$H$_{13}$N$_3$O (263.11): C, 72.99; H, 4.98; N, 15.96. Found: C, 73.04; H, 5.05; N, 16.10.

5.1.1.12. 3-Cyano-2-(2-naphthyl)-2*H*-indazole *N*^{1}-oxide (12). Yellow solid 0.71 g (75%) (method B); mp 218.3–220.0 °C (ethanol). ^{1}H NMR (400 MHz, CDCl$_3$) δ ppm: 7.46 (1H, dd, $J = 6.7$, 7.9 Hz), 7.51 (1H, dd, $J = 6.7$, 8.3 Hz), 7.68 (2H, m), 7.75 (1H, dd, $J = 2.0$, 8.8 Hz), 7.79 (1H, d, $J = 7.9$ Hz), 7.92 (1H, d, $J = 8.3$ Hz), 8.00 (1H, d, $J = 6.3$ Hz), 8.02 (1H, d, $J = 6.8$ Hz), 8.13 (1H, d, $J = 8.8$ Hz), 8.21 (1H, d, $J = 2.0$ Hz). ^{13}C NMR (100 MHz, CDCl$_3$) δ ppm: 92.60, 111.04, 115.08, 119.33, 123.5, 123.67, 127.48, 127.97, 128.03, 128.45, 128.90, 128.95, 129.18, 129.23, 129.60, 130.43, 133.29, 134.51. MS (EI, 70 eV) m/z (%): 285 (M$^+$, 14); 268 (M$^+$-17, 8); 179 (67); 144 (59); 127 (100); 115 (35). IR (KBr, cm^{-1}): 2207, 1489, 1435, 1339, 1248, 132, 855, 741. Anal. Calcd for C$_{18}$H$_{11}$N$_3$O (285.09): C, 75.78; H, 3.89; N, 14.73. Found: C, 75.46; H, 3.77; N, 14.59.

5.1.1.13. 3-Cyano-2-(1-naphthyl)-2*H*-indazole *N*[1]-oxide (13). Black solid 0.46 g (49%) (method B); mp 184.6–185.8 °C (ethanol). ^{1}H NMR (400 MHz, CDCl$_3$) δ ppm: 7.25 (1H, d, *J* = 8.0 Hz), 7.48 (1H, dd, *J* = 6.8, 8.0 Hz), 7.54 (1H, dd, *J* = 6.8, 8.0 Hz), 7.60 (1H, dd, *J* = 6.8, 8.0 Hz), 7.66 (1H, dd, *J* = 6.8, 8.4 Hz), 7.72 (1H, d, *J* = 4.2 Hz), 7.74 (1H, d, *J* = 5.4 Hz), 7.81 (1H, d, *J* = 8.0 Hz), 7.95 (1H, d, *J* = 8.0 Hz), 8.06 (1H, d, *J* = 8.4 Hz), 8.22 (1H, dd, *J* = 4.2, 5.4 Hz). ^{13}C NMR (100 MHz, CDCl$_3$) δ ppm: 92.00, 110.69, 115.25, 119.42, 122.32, 123.30, 125.59, 127.93, 128.04, 128.13, 128.18, 129.05, 129.21, 129.26, 129.50, 130.01, 133.41, 134.75. MS (EI, 70 eV) *m/z* (%): 285 (M[+], 100); 268 (M[+]-17, 9); 256 (39); 179 (47); 144 (17); 127 (62); 91 (25). IR (KBr, cm[−1]): 2209, 1487, 1458, 1381, 1262, 1059, 795, 774. Anal. Calcd for C$_{18}$H$_{11}$N$_3$O (285.09): C, 75.78; H, 3.89; N, 14.73. Found: C, 75.88; H, 3.68; N, 14.65.

5.1.2. Synthesis of indazole derivatives (16–18). *General method.* A mixture of the corresponding indazole *N*[1]-oxide (0.50 g, 1 equiv) (2, 5 and 6) and PPh$_3$ (1 equiv) in ethanol (30 mL) was heated at reflux for 5–6 h. Then the mixture was evaporated to dryness and the residue was purified by column chromatography and then crystallized from the indicated solvent.

5.1.2.1. 3-Cyano-2-(4-hydroxyphenyl)-2*H*-indazole (16). Yellow solid 0.22 g (46%); mp 177.9–181.0 °C (chloroform). ^{1}H NMR (400 MHz, DMSO-*d*$_6$) δ ppm: 7.03 (2H, d, *J* = 8.8 Hz), 7.43 (1H, dd, *J* = 6.8, 8.4 Hz), 7.53 (1H, dd, *J* = 6.8, 8.8 Hz), 7.72 (2H, d, *J* = 8.8 Hz), 7.90 (1H, d, *J* = 8.4 Hz), 7.97 (1H, d, *J* = 8.8 Hz), 10.21 (1H, br s). ^{13}C NMR (100 MHz, DMSO-*d*$_6$) δ ppm: 107.18, 112.27, 116.88, 119.32, 119.71, 126.76, 126.97, 127.02, 128.67, 131.14, 148.59, 159.91. MS (EI, 70 eV) *m/z* (%): 235 (M[+], 100); 206 (M[+]-30, 43); 193 (9); 179 (9); 65 (12). IR (KBr, cm[−1]): 3450–3230, 2220, 1590, 1430, 1345, 1035, 830, 750. Anal. Calcd for C$_{14}$H$_9$N$_3$O (235.07): C, 71.48; H, 3.86; N, 17.86. Found: C, 71.67; H, 3.55; N, 17.49.

5.1.2.2. 3-Cyano-2-(4-iodophenyl)-2*H*-indazole (17). Yellow solid 0.28 g (58%); mp 157.6–159.8 °C (ethanol). ^{1}H NMR (400 MHz, CDCl$_3$) δ ppm: 7.42 (1H, dd, *J* = 7.6, 8.4 Hz), 7.50 (1H, dd, *J* = 7.6, 8.4 Hz), 7.69 (2H, d, *J* = 8.8 Hz), 7.84 (1H, d, *J* = 8.4 Hz), 7.93 (1H, d, *J* = 8.4 Hz), 7.97 (2H, d, *J* = 8.8 Hz). ^{13}C NMR (100 MHz, CDCl$_3$) δ ppm: 95.91, 111.69, 119.07, 119.67, 125.67, 125.70, 126.98, 128.00, 128.67, 139.00, 139.34, 149.26. MS (EI, 70 eV) *m/z* (%): 239 (M[+]-I, 16); 218 (21); 179 (37); 81 (100); 53 (48). IR (KBr, cm[−1]): 2218, 1489, 1368, 1007, 824, 745. Anal. Calcd for C$_{14}$H$_8$IN$_3$ (344.98): C, 48.72; H, 2.34; N, 12.17. Found: C, 49.01; H, 2.56; N, 11.99.

5.1.2.3. 3-Cyano-2-(4-nitrophenyl)-2*H*-indazole (18). Yellow solid 0.17 g (37%); mp 180.7–182.5 °C (ethanol). ^{1}H NMR (400 MHz, DMSO-*d*$_6$) δ ppm: 7.52 (1H, dd, *J* = 6.8, 8.4 Hz), 7.60 (1H, dd, *J* = 6.8, 8.7 Hz), 7.97 (1H, d, *J* = 8.4 Hz), 8.03 (1H, d, *J* = 8.7 Hz), 8.27 (2H, d, *J* = 9.0 Hz), 8.56 (2H, d, *J* = 9.0 Hz). ^{13}C NMR (100 MHz, DMSO-*d*$_6$) δ ppm: 107.93, 111.45, 119.63, 119.95, 126.07, 126.18, 126.32, 127.76, 127.93, 129.76, 143.76, 149.35. MS (EI, 70 eV) *m/z* (%): 264 (M[+], 35); 217 (9); 164 (21); 140 (22); 122 (34); 105 (100). IR (KBr, cm[−1]): 2220, 1597, 1528, 1354, 857, 750. Anal. Calcd for C$_{14}$H$_8$N$_4$O$_2$ (264.06): C, 63.64; H, 3.05; N, 21.20. Found: C, 63.29; H, 2.94; N, 21.01.

5.2. Biology

5.2.1. Trypanocidal (epimastigotes) in vitro test. *Trypanosoma cruzi* epimastigotes (Brener or Tulahuen 2 strains) were grown at 28 °C in an axenic medium (BHI-Tryptose) as previously described,[9] complemented with 5% foetal bovine serum (FBS). Cells from a 10-day-old culture (stationary phase) were inoculated into 50 mL of fresh culture medium to give an initial concentration of 1×10^6 cells/mL. Cell growth was followed by measuring every day the absorbance of the culture at 600 nm. Before inoculation, the media were supplemented with the indicated amount of the drug from a stock solution in DMSO. The final concentration of DMSO in the culture media never exceeded 0.4% and the control was run in the presence of 0.4% DMSO and in the absence of any drug. No effect on epimastigote growth was observed by the presence of up to 1% DMSO in the culture media. The percentage of inhibition was calculated as follows: $\% = \{1 - [(A_p - A_{0p})/(A_c - A_{0c})]\} \times 100$, where $A_p = A_{600}$ of the culture containing the drug at day 5; $A_{0p} = A_{600}$ of the culture containing the drug just after addition of the inocula (day 0); $A_c = A_{600}$ of the culture in the absence of any drug (control) at day 5; $A_{0c} = A_{600}$ in the absence of the drug at day 0. To determine IC$_{50}$ values, 50% inhibitory concentrations, parasite growth was followed in the absence (control) and presence of increasing concentrations of the corresponding drug. At day 5, the absorbance of the culture was measured and related to the control. The IC$_{50}$ value was taken as the concentration of drug needed to reduce the absorbance ratio to 50%.

5.2.2. Trypanocidal (trypomastigotes) in vitro test[30]. Products were evaluated in vitro on the trypomastigote form of *T. cruzi* (CL Brener). BALB/c mice infected with *T. cruzi* were used 7 days after infection. Blood was obtained by cardiac puncture using 3.8% sodium citrate as anticoagulant in a 7:3 blood/anticoagulant ratio. The parasitaemia in infected mice ranged from 1×10^5 to 5×10^5 parasites/mL. The products were dissolved in minimal quantity of DMSO and added to PBS to give a final concentration of 100 and 250 µg/mL. Aliquots (10 µL) of each extract in triplicate were mixed in microtitre plates with 100 µL infected blood containing parasites at a concentration near to 10^6 parasites/mL. Infected blood and infected blood containing GV at 100 and 250 µg/mL concentration were used as control. The plates were shaken for 10 min at room temperature and kept at 4 °C for 24 h. Each solution was examined microscopically (OLYMPUS BH2) for parasite counting. The activity (% of parasites reduction) was compared with the standard drug GV.

5.2.3. Leishmanocidal in vitro test. The isolation, cultivation and maintenance of *Leishmania* promastigotes and

the technique used have been previously described.[31] Briefly, promastigote inhibition studies were performed on *L. amazonensis* (IFLA/BR/67/PH8), *L. infantum* (MHOM/ET/1967/L82,LV9) and *L. braziliensis* (MHOM/BR/75/M2903) grown at 25 °C in Schneider's drosophila medium containing 20% FBS. Compounds were dissolved in 40 µL DMSO (final concentration of this solvent 0.4%) or Tween 80, then diluted in the medium and placed in microtitre plates in triplicate, with a final compound concentration of 100 or 250 µg/mL. The microtitre plates of 96 bowls utilized contain 2×10^6 parasites/mL and the same proportion v/v with the product in each bowl. The activity of compounds was evaluated after 72 h by optical observation of a drop of each culture using an inverted microscope OLYMPUS IMT2 and comparison with control cell cultures and with those treated with the reference drug pentamidine. The evaluation is qualitative observing the lysis of parasites.

5.2.4. Antineoplastic assay. The compounds were tested at 10^{-4} M in the following tumour cell lines: MCF-7 (human mammary adenocarcinoma) (ATCC HTB-38), TK-10 (human kidney carcinoma) (NCI) and HT-29 (human colon adenocarcinoma) (ATCC HTB-38). The cytotoxicity test was carried out according to previously described procedures[32] with some modifications. *Cells.* An adequate cell suspension was prepared for each cell line (MCF-7, TK-10 or HT-29) in RPMI medium, supplemented with L-glutamine (1%), penicillin/streptomycin (1%), non-essential amino acids (1%) and 10% (v/v) FBS. Then, 225 µL was added into 96-well plates. The cultures were maintained at 37 °C and 5% CO_2 for 48 h. *Treatment.* Compound solutions were prepared just before dosing. Stock solutions, 1 mM, were prepared in 10% DMSO and 25 µL (final concentration 10^{-4} M) was added to each well. The cells were exposed for 24 h at 37 °C in 5% CO_2 atmosphere. *Measurement.* After exposure to the compound, the medium was eliminated and the cells were washed with PBS. The cells were fixed with 50 µL of trichloroacetic acid (50%) and 200 µL of culture medium (without FBS) for 1 h at 4 °C. Then, the cells were washed with purified water and treated with sulforhodamine B (0.4% wt/vol in 1% acetic acid) for 10 min at room temperature. The plates were washed with 1% acetic acid and dried overnight. Finally, 100 µL Tris buffer (pH 10.0) was added and absorbance at 540 nm was determined. *Calculations.* The cell survival percentage (SP) was calculated for all of the compounds as [(absorbance of cells post-treatment with product − absorbance of blank)/(absorbance of cells post-treatment with solvent − absorbance of blank)] × 100.

5.3. Cyclic voltammetry

Cyclic voltammetry was carried out using a Metrohm 693 VA instrument with a 694 VA Stand convertor and a 693 VA Processor, in DMSO (ca 1.0 mM), under a nitrogen atmosphere at room temperature, with tetrabutylammonium perchlorate (TBAP, ca 0.1 mM) as supporting electrolyte. Three-electrode cell was used where a mercury-dropping electrode as working electrode, a platinum wire as auxiliary electrode, and a saturated calomel as reference electrode were employed.

5.4. ESR experiments

NADPH, EDTA, DMPO and acetonitrile were obtained from Sigma. Incubations consisted of homogenized epimastigotes (Tulahuen 2 strain) of *T. cruzi* (4 mg protein/mL), NADPH (1 mM), EDTA (1 mM), DMPO (100 mM) in phosphate buffer, pH 7.4 (20 mM), and *N*-oxide derivative (2 mM) dissolved in acetonitrile. In all cases, NADPH was added immediately before the ESR spectrum was recorded. ESR spectra were recorded at room temperature in the X band (9.7 GHz) using a Bruker ECS 106 spectrometer with a rectangular cavity and 50 kHz field modulation. The hyperfine splitting constants were estimated to be accurate within 0.05.

5.5. Respiration experiments

Tulahuen strain *T. cruzi* epimastigotes were harvested by 500*g* centrifugation, followed by washing and re-suspension in 0.05 M sodium phosphate buffer, pH 7.4, and containing 0.107 M sodium chloride. Respiration measurements were carried out polarographically with a Clark No. 5331 electrode (Yellow Springs Instruments) in a 53 YSI model (Simpson Electric Co). The chamber volume was 2 mL and the temperature was 28 °C. The amount of parasite used was equivalent to 2 mg protein. The IC_{50} equivalent concentration corresponds to the final concentration used in the respiration experiments. This concentration was calculated considering that the IC_{50} (trypanocidal in vitro experiments) was determined using 3×10^6 parasites/mL, equivalent to 0.0375 mg protein/mL as initial parasite mass. Whereas 80×10^6 parasites/mL, equivalent to 1 mg protein/mL, was used in the respiration experiments. In order to maintain the parasite mass-drug ratio constant in these two types of experiments, the IC_{50} was corrected by this 26-fold parasite mass increase in the respiration experiment. Values are expressed as means ± SD for three independent experiments. No effect of DMSO alone was observed.

5.6. Crystallography study

The molecular structure of derivative **13**, $C_{18}H_{11}N_3O$, was determined by X-ray diffraction methods. The substance crystallizes in the monoclinic $P2_1/c$ space group, with $a = 8.024(1)$, $b = 20.186(3)$, $c = 8.692(1)$ Å, $\beta = 95.17(1)°$ and $Z = 4$. The structure was solved from 1840 reflections with $I > 2\sigma(I)$ and refined to agreement R1-factors of 0.050. The hydrogen atoms were positioned stereochemically and refined with the riding model. Intramolecular bond distances and angles, along with other crystallographic data, are given as Supporting information. Crystallographic data (excluding structure factors) for the structure in this paper have been deposited at the Cambridge Crystallographic Data Centre as supplementary publication numbers CCDC-284059. Copies of the data can be obtained, free of charge, on application to CCDC, 12 Union Road, Cambridge CB2 1EZ, UK [fax: 144-(0)1223-336033 or e-mail: deposit@ccdc.cam.ac.uk].

5.7. QSAR studies

The compounds were built with standard bond lengths and angles using the Spartan'04, 1.0.1 version,[24] suite of programs and the geometry of each molecule was fully optimized by applying semiempirical PM3 method in gas phase from the most stable conformer obtained using molecular mechanics (MMFF) methods. Angles and bond lengths of compound **13** were compared with the corresponding crystallographic data to validate the geometry optimization. Then, a single point calculation using density functional methodology (Becke's exchange functional (B) and Becke's three-parameter adiabatic connection (B3) hybrid exchange functional were used in combination with the Lee–Yang–Parr correlation functional).[33] The standard 6-31G* basis set of DZP quality was used for orbital expansion to solve the Kohn–Sham equations for first- and second-row elements. For heavier atoms a pseudopotential base (LACVP*) was used. Lipophilic properties of the compounds were included into the analyses, as $c\log P$ ($\log P$ calculated by the Villar method).

Supporting information

Crystallographic data for derivative **13** (five tables). Supplementary data associated with this article can be found, in the online version, at doi:10.1016/j.bmc.2006.01.007.

References and notes

1. Aldunate, J.; Morello, A. In *Free Radicals in Tropical Diseases*; Okezie, I., Ed.; University of London, 1993; p 137.
2. World Heath Organization: <http://www.who.int/ctd/chagas/burdens/>.
3. Cerecetto, H.; González, M. *Curr. Top. Med. Chem.* **2002**, *2*, 1187.
4. Urbina, J. A.; Docampo, R. *Trends Parasitol.* **2003**, *19*, 495.
5. <http://www.cdc.gov/ncidod/dpd/parasites/leishmania/> factsht leishmania; (b) <http://martin.parasitology.mcgill.ca/jimspage/biol/leish/>; (c) Cunningham, A. C. *Exp. Mol. Pathol.* **2002**, *72*, 132.
6. Croft, S. L.; Yardley, V. *Curr. Pharm. Des.* **2002**, *8*, 319.
7. (a) Grogl, M.; Thomason, T. N.; Franke, E. D. *Am. J. Trop. Med. Hyg.* **1992**, *47*, 117; (b) Sanders, J. M.; Ortiz, A.; Mao, J.; Meints, G. A.; Van Brussel, E. M.; Burzynska, A.; Kafarski, P.; González-Pacanowska, D.; Oldfield, E. *J. Med. Chem.* **2003**, *46*, 5171.
8. (a) Arán, V. J.; Ochoa, C.; Boiani, L.; Buccino, P.; Cerecetto, H.; Gerpe, A.; González, M.; Montero, D.; Nogal, J. J.; Gómez-Barrio, A.; Azqueta, A.; López de Ceráin, A.; Piro, O. E.; Castellano, E. E. *Bioorg. Med. Chem.* **2005**, *13*, 3197; (b) Olea-Azar, C.; Cerecetto, H.; Gerpe, A.; González, M.; Arán, V. J.; Rigol, C.; Opazo, L. *Spectrochim. Acta Part A* **2005**, *63*, 36–42.
9. (a) Cerecetto, H.; Di Maio, R.; González, M.; Risso, M.; Saenz, P.; Seoane, G.; Denicola, A.; Peluffo, G.; Quijano, C.; Olea-Azar, C. *J. Med. Chem.* **1999**, *42*, 1941; (b) Aguirre, G.; Cerecetto, H.; Di Maio, R.; González, M.; Seoane, G.; Denicola, A.; Ortega, M. A.; Aldana, I.; Monge, A. *Arch. Pharm.* **2002**, *335*, 15; (c) Aguirre, G.; Boiani, M.; Cerecetto, H.; Gerpe, A.; González, M.; Fernández, Y.; Denicola, A.; Ochoa, C.; Nogal, J. J.; Montero, D.; Escario, J. A. *Arch. Pharm. Med. Chem.* **2004**, *337*, 259; (d) Aguirre, G.; Boiani, L.; Cerecetto, H.; Di Maio, R.; González, M.; Porcal, W.; Thomson, L.; Tórtora, V.; Denicola, A.; Moler, M. *Bioorg. Med. Chem.* **2005**, *13*, 6324; (e) Aguirre, G.; Boiani, L.; Boiani, M.; Cerecetto, H.; Di Maio, R.; González, M.; Porcal, W.; Denicola, A.; Piro, O. E.; Castellano, E. E.; Sant'Anna, M.; Barreiro, E. *J. Bioorg. Med. Chem.* **2005**, *13*, 6336.
10. (a) Elwell, J. H.; Siim, B. G.; Evans, J. W.; Brown, J. M. *Biochem. Pharmacol.* **1997**, *54*, 249; (b) Cerecetto, H.; González, M. *Mini-Rev. Med. Chem.* **2001**, *1*, 219.
11. (a) Behr, L. C. *J. Org. Chem.* **1954**, *76*, 3672; (b) Behr, L. C.; Alley, E. G.; Levand, O. *J. Org. Chem.* **1962**, *27*, 65.
12. Johnston, D.; Smith, D. M.; Shepherd, T.; Thompson, D. *J. Chem. Soc., Perkin Trans. I* **1987**, 495.
13. Zenchoff, G. S.; Walser, A.; Fryer, R. I. *J. Heterocyclic Chem.* **1976**, *13*, 33.
14. (a) Howard, E.; Olszewski, W. F. *J. Am. Chem. Soc.* **1959**, *81*, 1483; (b) Boyer, J. H.; Ellzey, S. E. *J. Org. Chem.* **1961**, *26*, 4684; (c) Ghosh, P. B.; Whitehouse, M. W. *J. Med. Chem.* **1968**, *11*, 305.
15. (a) In derivative **13**, the indazole ring is planar. The 3-cyano-2*H*-indazole N^1-oxide plane is nearly perpendicular to the naphthalene substituent. The N–O bonding to the indazole heterocycle ring produces a slight lengthening of the adjacent N–C and N–N bonds (atomic coordinates, bond distances and angles, crystal data, data collection procedure, structure determination method and refinement results are given as Supplementary information).(b) Enraf-Nonius (1997–2000). COLLECT. Nonius BV, Delft, The Netherlands. K. Harms and S. Wocadlo, XCAD4 – CAD4 Data Reduction., University of Marburg, Marburg, Germany, 1995.; (c) PLATON, A Multipurpose Crystallographic Tool, Utrecht University, Utrecht, The Netherlands, A. L. Spek, 1998; (d) Sheldrick, G. M. *SHELXS-97. Program for Crystal Structure Resolution*; University of Göttingen: Göttingen, Germany, 1997; (e) Sheldrick, G. M. *SHELXL-97. Program for Crystal Structures Analysis*; University of Göttingen: Göttingen, Germany, 1997; (f) Johnson, C. K. *ORTEP-II. A Fortran Thermal-Ellipsoid Plot Program. Report ORNL-5138*; Oak Ridge National Laboratory: Tennessee, USA, 1976.
16. Enanga, B.; Keita, M.; Chauviere, G.; Dumas, M.; Bouteille, B. *Trop. Med. Int. Health* **1998**, *3*, 736.
17. (a) Maya, J. D.; Bollo, S.; Nuñez-Vergara, L. J.; Squella, J. A.; Repetto, Y.; Morello, A.; Périé, J.; Chauviere, G. *Biochem. Pharmacol.* **2003**, *65*, 999; (b) Olea-Azar, C.; Atria, A. M.; Mendizábal, F.; Di Maio, R.; Seoane, G.; Cerecetto, A. M. *Spectrosc. Lett.* **1998**, *31*, 99; (c) Olea-Azar, C.; Rigol, C.; Mendizabal, F.; Morello, A.; Maya, J. D.; Moncada, C.; Cabrera, E.; Di Maio, R.; González, M.; Cerecetto, H. *Free Radic. Res.* **2003**, *37*, 993.
18. Nuñez-Vergara, L. J.; Bonta, M.; Navarrete-Encina, P. A.; Squella, J. A. *Electrochim. Acta* **2001**, *46*, 4289.
19. (a) The number of electrons, *n*, was determined from the slope of the graphic E_{pc} versus sweep rates, *v*, using the relationship $E_{pc} = k - (RT/\alpha nF)$ Ln *v* considering α equal

to 0.5. The same values of n were obtained from the slope of the graphic intensity, I, versus E_{pc} using the relationship $I = k - (\alpha nF/RT)\, E_{pc}$ considering α equal to 0.5; (b) Bord, A. J.; Faulkner, L. R. In *Electrochemical Methods. Fundamentals and Applications*; Wiley: New York, 1980.

20. Núñez-Vergara, L. J.; Squella, J. A.; Olea-Azar, C.; Bollo, S.; Navarrete-Encina, P. A.; Sturm, J. C. *Electrochim. Acta* **2000**, *45*, 3555.
21. René, K.; Vacek, J.; Trnková, L.; Frantisek, J. *Bioelect-rochemistry* **2004**, *63*, 19.
22. (a) Olea-Azar, C.; Rigol, C.; Opazo, L.; Morello, A.; Maya, J. D.; Repetto, Y.; Aguirre, G.; Cerecetto, H.; Di Maio, R.; González, M.; Porcal, W. *J. Chil. Chem. Soc.* **2003**, *48*, 77; (b) Lai, C.; Grover, T. A.; Piette, L. H. *Arch. Biochem. Biophys.* **1979**, *193*, 373.
23. (a) Hehre, W. J.; Radom, L.; Schleyer, P. V. R.; Pople, J. A. In *Ab Initio Molecular Orbital Theory*; Wiley: New York, 1986; (b) Hehre, W. J.; Shusterman, A. J.; Huang, W. W. *A Laboratory Book of Computational Organic Chemistry*; Wavefunction: California, 1996; (c) Hehre, W. J. *A Guide to Molecular Mechanics and Quantum Chemical Calculations*; Wavefunction: California, 2003.
24. (a) Wavefunction, Inc. 18401 Von Karman Avenue, Suite 370. Irvine, California 92612 USA.; (b) PC Spartan Pro User's Guide, Wavefunction Inc., California, **1999**.
25. Squared correlation matrix of descriptors used in the QSAR study.

μ	1			
E_{HOMO}	0.895	1		
cLogP	0.042	0.103	1	
vol	0.003	0.020	0.749	1
r^2	μ	E_{HOMO}	cLogP	vol

26. (a) Myers, R. H. *Classical and Modern Regression with Application*; P.W.S. Publishers: Boston, 1986; (b) Daniel, C.; Wood, F. S. In *Fitting Equations to Data*, 2nd ed.; Wiley: New York, 1980; (c) Draper, N. R.; Smith, H. In *Applied Regression Analysis*, 2nd ed.; Wiley: New York, 1981.
27. (a) Cerecetto, H.; Dias, E.; Di Maio, R.; González, M.; Pacce, S.; Saenz, P.; Seoane, G.; Suescun, L.; Mombrú, A.; Fernández, G.; Lema, M.; Villalba, J. *J. Agric. Food Chem.* **2000**, *48*, 2995; (b) Boiani, M.; Cerecetto, H.; González, M.; Risso, M.; Olea-Azar, C.; Piro, O. E.; Catellano, E. E.; López de Ceráin, A.; Ezpeleta, O.; Monge-Vega, A. *Eur. J. Med. Chem.* **2001**, *36*, 771.
28. Dhainaut, A.; Tizot, A.; Raimbaud, E.; Lockart, B.; Lestage, P.; Goldstein, S. *J. Med. Chem.* **2000**, *43*, 2165.
29. (a) Hansch, D.; Unger, S. H.; Forsythe, A. B. *J. Med. Chem.* **1973**, *16*, 1217; (b) Hansch, C.; Leo, A. In *Substituent Constants for Correlation Analysis in Chemistry and Biology*; Wiley: New York, 1979.
30. Rojas de Arias, A.; Fournet, A.; Inchausti, A.; Ascurra, M.; Fleitas, N.; Rodríguez, E. *Phytotherapy Res.* **1994**, *8*, 141.
31. Fournet, A.; Ferreira, M.; Rojas de Arias, A.; Fuentes, S.; Torres, S.; Inchausti, A.; Yaluff, G.; Nakayama, H.; Mahiou, V.; Hocquemiller, R.; Cave, A. *Phytomedicine* **1996**, *11*, 271.
32. Monks, A.; Scudiero, D.; Skehan, P.; Shoemaker, R.; Paull, K.; Vistica, D.; Hose, C.; Langley, J.; Cronise, P.; Vaigro-Wolff, A.; Gray-Goodrich, M.; Campbell, H.; Mayo, J.; Boyd, M. *J. Natl. Cancer Inst.* **1991**, *83*, 757.
33. (a) Becke, A. D. *Phys. Rev. A.* **1988**, *38*, 3098; (b) Becke, A. D. *J. Chem. Phys.* **1993**, 5648; (c) Lee, C.; Yang, W.; Parr, R. G. *Phys. Rev. B. Condens. Matter* **1988**, *37*, 785.